Collapse of the Josephson Emission in a Carbon Nanotube Junction in the Kondo Regime

D. Watfa,[1] R. Delagrange,[1] A. Kadlecová,[2] M. Ferrier,[1] A. Kasumov,[1] H. Bouchiat,[1] and R. Deblock[1]

[1]*Université Paris-Saclay, CNRS, Laboratoire de Physique des Solides, 91405 Orsay, France*
[2]*Department of Condensed Matter Physics, Faculty of Mathematics and Physics, Charles University,*
Ke Karlovu 5, CZ-121 16 Praha 2, Czech Republic

We probe the high frequency emission of a carbon nanotube based Josephson junction and compare it to its dc Josephson current. The ac emission is probed by coupling the carbon nanotube to an on-chip detector (a superconductor-insulator-superconductor junction), via a coplanar waveguide resonator. The measurement of the photoassisted current of the detector gives direct access to the signal emitted by the carbon nanotube. We focus on the gate regions that exhibit Kondo features in the normal state and demonstrate that when the dc supercurrent is enhanced by the Kondo effect, the ac Josephson effect is strongly reduced. This result is compared to numerical renormalization group theory and is attributed to a transition between the singlet ground state and the doublet excited state which is enabled only when the junction is driven out-of-equilibrium by a voltage bias.

The ac Josephson effect [1] is the phenomenon by which a superconducting weak link with a bias voltage V generates an oscillating current at frequency $\nu_J = 2\,eV/h$. It has been used to explore the Andreev bound states (ABS) spectrum, which determines the supercurrent carried by the junction. For instance, its measurement points toward the topologically protected crossing of ABS in HgTe [2,3], InAs nanowires [4], and Dirac semimetals [5]. However, when probing the ac Josephson effect, due to the applied voltage bias and the resulting time evolution of the superconducting phase, the junction is driven out-of-equilibrium. This changes the occupation of the Andreev levels and the dynamics of the quasiparticles (QP) in the system [6,7] and can lead to new physical effects not accessible at equilibrium.

In the present Letter, we explore this out-of-equilibrium situation in a Josephson junction based on a carbon nanotube (CNT) quantum dot (QD) in the Kondo regime. In such a junction, without Kondo effect, electron-electron interaction results in Coulomb blockade, which gives rise to a doublet spin 1/2 state if there is an odd number of electrons on the dot. In this doublet state, the Cooper pairs pass through the QD thanks to sequential cotunneling processes that involve a spin flip. This manifests as a reduced critical current and a π shift of the current-phase relation [8–11], called π junction. However, due to the coupling to the reservoirs and local interactions, Kondo correlations can develop. The Kondo effect is a many-body interaction between a localized impurity spin and free conduction electrons leading to the screening of the impurity spin [12–14]. By enhancing cotunneling processes, a Kondo resonant state arises that is able to overcome the Coulomb blockade by opening a perfectly transmitted

channel through the quantum dot when connected to normal reservoirs. For superconducting reservoirs, if the Kondo temperature is larger than the superconducting gap ($k_B T_K > \Delta$), the Kondo effect and the superconductivity cooperate and enhance the dc Josephson effect by restoring the spin 0 singlet state (0-junction behavior).

This singlet to doublet transition in QDs has attracted a large theoretical interest (see the recent review [15]). Experimentally, it is now well established that it can be driven by the gate voltage [11,16], the magnetic field [17], and the superconducting phase [18,19]. Here, we explore this transition by using the measurement of the Josephson emission as a probe of the state of the junction and find a range of parameters where this transition is forbidden at equilibrium but enabled when the junction is driven out-of-equilibrium by a voltage bias.

The Josephson emission of the CNT-based Josephson junction is probed using an on-chip detection scheme. In the gate regions that exhibit Kondo features in the normal state, the supercurrent is found to be enhanced by the Kondo effect, whereas the Josephson emission is found to be strongly reduced such that the ac emission is not proportional to the dc supercurrent, as it could be naively expected from the Josephson relations. This striking result strongly suggests a dynamical change in the state of the junction, from singlet to doublet, induced by the phase evolution of the junction and the quasiparticle dynamics in the QD.

The CNT Josephson junction is coupled to an on-chip detector, a superconductor-insulator-superconductor (SIS) junction [20–22], via a coplanar waveguide resonator [Fig. 1(a)]. The CNTs are grown by chemical vapor deposition on an oxidized undoped silicon substrate [23]. The
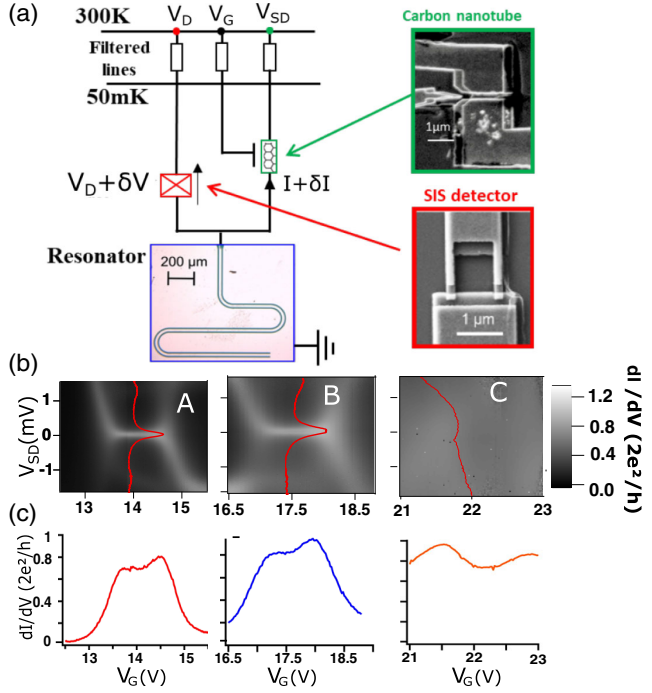
FIG. 1. Sample and normal state characterization. (a) The CNT Josephson junction is coupled to a SIS junction via a coplanar waveguide resonator. (b) Differential conductance dI/dV_{SD} as a function of source-drain (SD) bias voltage V_{SD} and gate voltage V_G for Kondo ridges A and B and zone C. dI/dV_{SD} curves taken at gate voltages 14, 17.5, and 21.5 V are shown on top of the color plot (red curves). (c) Conductance at $V_{SD} = 0$ of Kondo ridges A and B, and for zone C.

contacts to the tube, the detector, and the resonant circuit are made using electron beam lithography and metal deposition. The contacts are 400 nm apart and made of Pd(7 nm)/Al(100 nm) ($\Delta = 50\ \mu eV$) or Pd(80 nm)/Nb(11 nm)/Al(50 nm) ($\Delta = 150\ \mu eV$). Pd provides good contact to the CNTs, however, reduces Δ compared to bare Al or Nb. Superconductivity in the Pd/Al contact is suppressed by a low magnetic field of 0.1 T, without affecting the normal state of the CNT, allowing a good determination of the parameters of the dots. However, for the Pd/Nb/Al contacts, the needed magnetic field is at least 1 T, thus, preventing a reliable extraction of all the dot parameters. The sample is cooled down in a dilution refrigerator of base temperature 50 mK and measured through low-pass filtered lines. The differential conductance is probed with a lock-in technique.

When biased by a voltage V_{SD}, the CNT emits photons at the Josephson frequency $\nu_J = 2eV_{SD}/h$. The SIS detector absorbs those photons, inducing a photoassisted tunneling (PAT) current I_{PAT}. The resonant coupling circuit between detector and CNT transmits only at the resonance frequencies, designed to be $\nu_0 = 12.5$ GHz and odd harmonics. The I_{PAT} current through the detector, biased at V_D such that $2\Delta - h\nu < V_D < 2\Delta$, is proportional to the amplitude of the ac Josephson emission I_C^{ac}, following the relation [22]

$$I_{PAT} = \frac{1}{(2V_{SD})^2}\frac{(I_C^{ac})^2}{4}|Z_t(2\ eV_{SD}/h)|^2 I_{qp}^0(V_D + 2V_{SD}),$$

$$(1)$$

with $I_{qp}^0(V_D)$, the IV characteristic of the detector without irradiation and $Z_t(\nu)$, the impedance of the resonant circuit at frequency ν. I_{PAT} is obtained experimentally as the dc current in the SIS detector, and allows us to extract I_C^{ac} using Eq. (1) (see Supplemental Material [24]).

The CNT with Pd/Al contacts is characterized first in the normal state. The differential conductance dI/dV_{SD} of the CNT is measured as a function of the bias voltage (V_{SD}) and the gate voltage (V_G) [see Fig 1(b)]. The stability diagram of the QD exhibits Coulomb blockade diamonds with the fourfold degeneracy found for clean CNT QDs. In the diamonds with odd number of electrons, the Kondo effect manifests through a high conductance region at zero bias, the Kondo ridge. We focus on two Kondo ridges A and B, with filling $N = 1$ and $N = 3$, respectively. In Figs. 1(b)–1(c), we also show another gate region, called, hereafter, region C, with a conductance close to the conductance quantum but without Kondo features. We consider, as well, a similar Kondo ridge in the sample with Pd/Nb/Al contacts, that we call region D [24]. The different parameters of the QD (see Table I), described with the single impurity Anderson model, are extracted for the Kondo ridges A and B. The charging energy U is deduced from the size of the Coulomb diamond, the asymmetry $a = \Gamma_L/\Gamma_R$ of the contact from the value of the zero-bias conductance at the particle-hole symmetry point, and the coupling to the reservoirs $\Gamma = \Gamma_L + \Gamma_R$ from the gate dependence of the Kondo temperature T_K [24].

Now, we turn to the superconducting regime where a supercurrent can flow through the junction. The differential resistance dV_{SD}/dI is measured as a function of the bias current I and V_G [Fig. 2(a)]. We use the resistively and capacitively shunted junction (RCSJ) model [10,44,45] to model the electromagnetic environment of the junction and account for a dissipative Josephson branch [24]. From this model, we extract the value of the critical current I_c and the resistance of the junction R_J [Figs. 2(b)–2(d)]. The three regions A, B, and C exhibit a gate modulated critical current and resistance R_J. $1/R_J$ behaves quite similarly to the measured conductance in the superconducting regime

TABLE I. Parameters of the CNT QD in the three Kondo regions considered in this Letter. Because of the high critical field of the Pd/Nb/Al contacts, the Kondo region D could not be fully characterized.

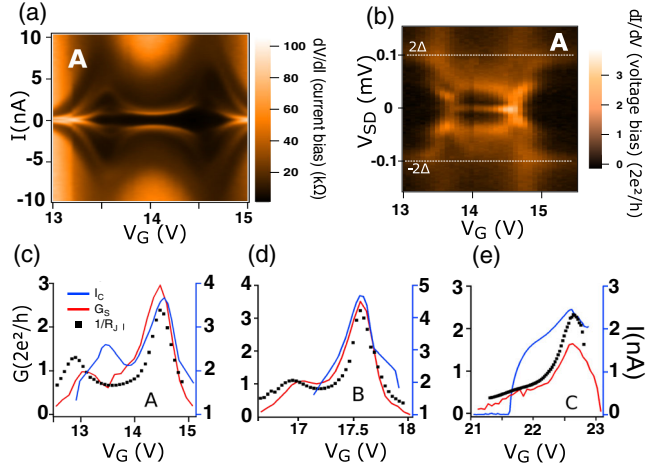|	$T_K(K)$	U (meV)	Γ (meV)	a	Δ (meV)
Kondo A	1.1	3.9	0.62	3.3	0.05
Kondo B	1.7	4	0.75	2.5	0.05
Kondo D	$> \Delta$	2			0.15

FIG. 2.   dc Josephson effect. (a) Differential resistance dV_{SD}/dI of the CNT Josephson junction as a function of the bias current I and V_G for Kondo ridge A. (b) Differential conductance dI/dV_{SD} of the CNT Josephson junction as a function of V_{SD} and V_G for Kondo ridge A. (c)–(e) Gate dependence for regions A, B, and C of the critical current I_C (blue curve) and the inverse of the resistance R_J (square dots) extracted from the RCSJ model (see text and [24]). $G_S = dI/dV_{SD}$ at zero bias is plotted as the red line.

FIG. 3.   Josephson emission. (a) PAT current in the detector as a function of V_{SD} and V_G for zone A. (b)–(d) Comparison of the critical current I_C and the ac critical current I_C^{ac} for zones A, B, and C. (e) Same comparison for the sample with Pd/Nb/Al contact and two resonator modes ($\nu_0 = 11$ and $\nu_1 = 31$ GHz). The curve for the critical current has to be multiplied by 10.

G_S. The fact that the critical current in the Kondo regions A and B remains relatively large is a good indicator that the QD stays in the singlet state, leading to a 0-junction behavior. This is expected from the ratio $k_B T_K/\Delta$ and the asymmetry [46,47]. The same qualitative behavior is seen on sample with Pd/Nb/Al contacts, where the Josephson branch is less dissipative and allows direct extraction of I_c, without using the RCSJ model [24].

We have performed numerical renormalization group (NRG) calculations [48,49] of the energy spectrum and supercurrent [Figs. 4(a)–4(c)] using the parameters determined in the normal state (Table I). They confirm that the ground state of the system for regions A and B is always the singlet state. This leads to a supercurrent in the nanoampere range, consistent with the experiment, with the phase behavior of a 0 junction.

To measure the Josephson emission, we voltage bias the detector such that $2\Delta - h\nu_0 < |V_D| < 2\Delta$ and measure simultaneously dI/dV_{SD} [Fig. 2(b)] and the PAT current [Fig. 3(a)] as a function of V_G and V_{SD}. In Fig. 2(b), the conductance of the sample shows the onset of QP tunneling at $V_{SD} = \pm 0.1$ mV, corresponding to $\Delta = 50 \mu eV$. There is a strong increase of conductance at zero bias due to the supercurrent branch. Below the superconducting gap, finite conductance features are related to multiple Andreev reflection (MAR) processes.

In Fig. 3(a), the PAT current reveals that the emission of the CNT junction has two contributions. One is the ac Josephson effect of the junction, at the Josephson frequency $\nu_J = 2 eV_{SD}/h$. The second contribution is
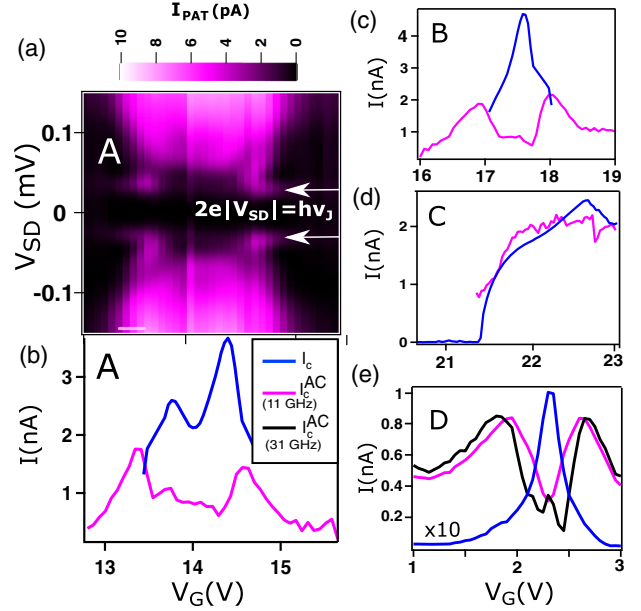
broadband and associated to MAR processes and QP tunneling. In the PAT response, we do not detect any signature of harmonics in the ac Josephson effect (expected at voltage $V_{SD} = h\nu_J/2ne$ for the nth harmonics). Consequently, we separate the two processes by attributing the peak at ν_J to the ac Josephson effect and the remaining baseline to the broadband contribution (see Fig. 4 of [24]). In Figs. 3(b)–3(e), the amplitude of the dynamical critical current I_C^{ac} is plotted, extracted using formula (1) from the peak at $V_{SD} = h\nu/(2e)$ in the PAT current. In the reference region C, where there is neither Coulomb blockade nor Kondo effect, this dynamical critical current follows the dc critical current I_C. By contrast, close to the center of the Kondo regions A, B, and D, there is a strong reduction of I_C^{ac}, in a region where the critical current I_C is enhanced due to the Kondo correlations [Figs. 3(b)–3(e)]. In region D, this effect could be observed, as well, at the 31 GHz mode of the resonator, and is even enhanced compared to the fundamental frequency [Fig. 3(e)]. This collapse of the ac Josephson emission, enhanced as the Josephson frequency increases and specific to the Kondo regions, is the central result of this work.

Now, we turn to possible explanations for the reduction of the ac Josephson effect in the Kondo regime. One may think about the decoherence of the Kondo effect due to voltage induced spin relaxation [50–54], or dynamical effects similar to the high-frequency cutoff for the emission of a quantum dot in the normal state [21].
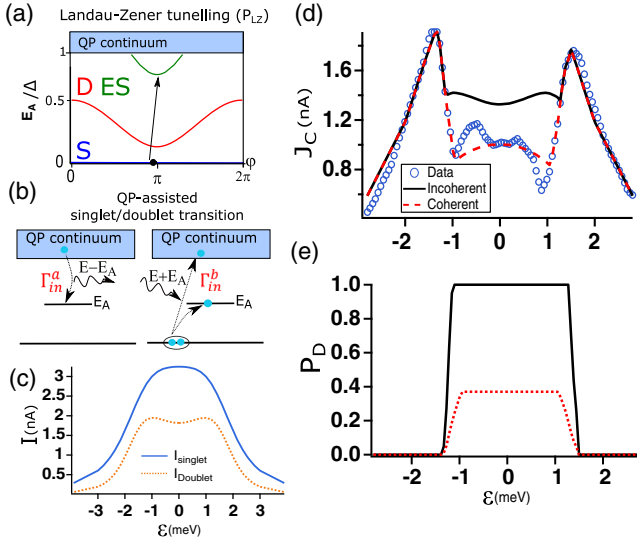
FIG. 4.   (a) NRG many-body spectrum as a function of the superconducting phase φ at the particle-hole symmetry point for the Kondo ridge A. The ground state is singlet (S), the first excited state a doublet (D, red curve), and the second excited state a singlet (ES, green curve). The arrow illustrates the Landau-Zener process, where the system tunnels from S to ES. (b) Illustration of two QP-assisted processes to excite the doublet state (D), associated with energy exchange with the environment. (c) Calculated amplitude of the first harmonics of the current phase relation for zone A in the singlet and doublet state. (d) Comparison between the data for Kondo ridge A (blue circles) and the calculated amplitude of the ac supercurrent I_C^{ac} introducing a finite probability P_D for the system to be in the doublet state using incoherent (black solid line) and coherent (red dashed line) scenarios (see text) (e) P_D in the incoherent (black solid line) and coherent (red dashed line) regimes.

However, because $eV_{SD}/k_B T_K < 1$, $h\nu_J/k_B T_K < 1$ and the asymmetry of the coupling to the contacts, these effects shall remain small.

Another possible process is Landau-Zener (LZ) tunneling, that induces a transition to excited levels with a probability which increases when the phase velocity (and thus, the Josephson frequency) is high. This is what happens for a quantum channel junction with high transparency ([24,55]) and involves transitions between singlet states, due to parity constraints [56]. However, for the quantum dot, the energy of the excited singlet state is rather close to Δ [see Fig. 4(a)]. The probability P_{LZ} of this transition, while not completely negligible ($P_{LZ} = 0.43$), depends little on V_G [24]. This would not account for the suppression of the ac Josephson emission observed in Fig. 3.

The collapse of the Josephson emission is more likely related to transitions from the ground state singlet to the doublet state. This is made possible by the tunneling of QP in the QD thanks to energy exchange with the environment, also called QP poisoning [see Fig. 4(b)]. First, we consider the situation where no bias voltage is applied, and find that the probability P_D for the QD to be in the doublet state is

small in a dc current configuration with a current bias varying in the kilohertz range ([24,57]). This explains why the measurement of the dc critical current, which happens at the maximum of the supercurrent around $\varphi = \pi/2$, is consistent with a 0-junction and a singlet ground state.

The situation can be quite different when one measures the ac emission. The theory for QD in this regime is not available, except for particular limits [58–60], and we give the following qualitative arguments. Because of the applied bias needed to have Josephson emission, the QP injection rate Γ_{in} increases significantly compared to equilibrium. Moreover, close to the particle-hole symmetry point, the doublet state is detached from the continuum with a relatively large gap Δ_{cont}. This keeps the escape rate of QPs relatively low, while the injection rate is increased, such that the probability for the QD to be in the doublet state is expected to be higher in a voltage biased situation. This leads to a decrease of I_{ac}^C since the critical current of the doublet state is lower than the one of the singlet ground state. Despite a higher gap value, the samples with Pd/Nb/Al contacts exhibit the same phenomenon [Fig. 3(e)]. This can be related to the existence of a soft gap for these samples, inducing a small but finite QP density at energy below the gap.

Moving away from the electron-hole symmetry point, Δ_{cont} is reduced significantly (Fig. 11 of [24]), which increases the probability for a QP present on the dot to escape thanks to Demkov Osherov tunneling processes between the doublet state and the continuum ([24,42,61,62]. Concurrently, the minimum value of energy of the doublet state, at $\varphi = \pi$, increases, which reduces the rate of QP injection into the QD. Thus, these two effects restore a high probability for the QD to be in the singlet ground state and increases its effective supercurrent. That is what is measured in the experiment.

From the amplitude of the ac emission, it is possible to extract P_D assuming that the dynamical Josephson current is given by $I_{ac}^C = P_D J_D + (1 - P_D)J_S$, where J_S is the amplitude of the critical current in the singlet state and J_D the one in the doublet state [Fig. 4(c)]. In an incoherent scenario, where the QP dynamics is not correlated with the phase evolution of the junction, only the absolute value of the amplitude of the singlet and doublet supercurrent is taken into account. With a probability one to be in the doublet state close to the particle-hole symmetry point, one can qualitatively reproduce the reduction of the supercurrent [Figs. 4(d) and 4(e)]. Oppositely, in a coherent scenario, where the QP dynamics is correlated with the phase evolution of the junction, the sign of the supercurrent (positive for the singlet and negative for the doublet) has to be considered. This leads to a quantitative agreement with the data [Figs. 4(d) and 4(e)], with a finite probability of being in the doublet state, but puts a strong constraint on the model used to describe the dynamics of the junction.

To conclude, we have explored the singlet to doublet transition of an out-of-equilibrium CNT Josephson junction by probing its Josephson emission. It is strikingly reduced in the gate regions where the critical current is enhanced due to the interplay of the Kondo effect and the superconducting proximity effect. We interpret this result as a transition between a singlet ground state and a doublet excited state induced by the dynamics of quasiparticles in the QD. Thus, this demonstrates the importance of taking into account electron-electron interactions and nonequilibrium processes to understand the dynamics of QD Josephson junctions.

[1] B. D. Josephson, Phys. Lett. **1**, 251 (1962).
[2] J. Wiedenmann *et al.*, Nat. Commun. **7**, 10303 (2016).
[3] R. S. Deacon *et al.*, Phys. Rev. X **7**, 021011 (2017).
[4] D. Laroche *et al.*, Nat. Commun. **10**, 245 (2019).
[5] C. Li, J. C. de Boer, B. de Ronde, S. V. Ramankutty, E. van Heumen, Y. Huang, A. de Visser, A. A. Golubov, M. S. Golden, and A. Brinkman, Nat. Mater. **17**, 875 (2018).
[6] J. Basset, M. Kuzmanović, P. Virtanen, T. T. Heikkilä, J. Estève, J. Gabelli, C. Strunk, and M. Aprili, Phys. Rev. Research **1**, 032009(R) (2019).
[7] P.-M. Billangeon, F. Pierre, H. Bouchiat, and R. Deblock, Phys. Rev. Lett. **98**, 216802 (2007).
[8] J. A. van Dam, Y. V. Nazarov, Erik P. A. M. Bakkers, S. De Franceschi, and L. P. Kouwenhoven, Nature (London) **442**, 667 (2006).
[9] J.-P. Cleuziou, W. Wernsdorfer, V. Bouchiat, T. Ondarçuhu, and M. Monthioux, Nat. Nanotechnol. **1**, 53 (2006).
[10] H. I. Jørgensen, T. Novotný, K. Grove-Rasmussen, K. Flensberg, and P. E. Lindelof, Nano Lett. **7**, 2441 (2007).
[11] S. De Franceschi, L. Kouwenhoven, C. Schönenberger, and W. Wernsdorfer, Nat. Nanotechnol. **5**, 703 (2010).
[12] M. Pustilnik and L. Glazman, J. Phys. Condens. Matter **16**, R513 (2004).
[13] D. Goldhaber-Gordon, J. Göres, M. A. Kastner, H. Shtrikman, D. Mahalu, and U. Meirav, Phys. Rev. Lett. **81**, 5225 (1998).
[14] S. M. Cronenwett, T. H. Oosterkamp, and L. P. Kouwenhoven, Science **281**, 540 (1998).
[15] V. Meden, J. Phys. Condens. Matter **31**, 163001 (2019).
[16] R. Maurand, T. Meng, E. Bonet, S. Florens, L. Marty, and W. Wernsdorfer, Phys. Rev. X **2**, 011009 (2012).
[17] A. García Corral, D. M. T. van Zanten, K. J. Franke, H. Courtois, S. Florens, and C. B. Winkelmann, Phys. Rev. Research **2**, 012065(R) (2020).
[18] R. Delagrange, D. J. Luitz, R. Weil, A. Kasumov, V. Meden, H. Bouchiat, and R. Deblock, Phys. Rev. B **91**, 241401(R) (2015).
[19] R. Delagrange, R. Weil, A. Kasumov, M. Ferrier, H. Bouchiat, and R. Deblock, Phys. Rev. B **93**, 195437 (2016).
[20] R. Deblock, E. Onac, L. Gurevich, and L. P. Kouwenhoven, Science **301**, 203 (2003).
[21] R. Delagrange, J. Basset, H. Bouchiat, and R. Deblock, Phys. Rev. B **97**, 041412(R) (2018).
[22] J. Basset, H. Bouchiat, and R. Deblock, Phys. Rev. Lett. **105**, 166801 (2010).
[23] Y. Kasumov *et al.*, Appl. Phys. A **88**, 687 (2007).
[24] See Supplemental Material at http://link.aps.org/supplemental/10.1103/PhysRevLett.126.126801 for a discussion of the extraction of Kondo temperature and parameters of the quantum dot, the critical current, the measurement of the PAT current and ac emission, a presentation of data for other samples, details on NRG calculation of the Andreev spectrum and the supercurrent, a comparison of quantum dot and quantum channel Josephson junctions, and finally, the evaluation of the quasiparticle dynamics in the QD junction, which includes Refs. [25–43].
[25] A. M. Tsvelick and P. B. Wiegmann, Adv. Phys. **32**, 453 (1983).
[26] N. E. Bickers, Rev. Mod. Phys. **59**, 845 (1987).
[27] B. Babić, T. Kontos, and C. Schönenberger, Phys. Rev. B **70**, 235419 (2004).
[28] T. S. Jespersen, M. Aagesen, C. Sørensen, P. E. Lindelof, and J. Nygård, Phys. Rev. B **74**, 233304 (2006).
[29] A. V. Kretinin, H. Shtrikman, D. Goldhaber-Gordon, M. Hanl, A. Weichselbaum, J. von Delft, T. Costi, and D. Mahalu, Phys. Rev. B **84**, 245316 (2011).
[30] T. A. Costi, A. C. Hewson, and V. Zlatic, J. Phys. Condens. Matter **6**, 2519 (1994).
[31] S. Sasaki, S. Amaha, N. Asakawa, M. Eto, and S. Tarucha, Phys. Rev. Lett. **93**, 017205 (2004).
[32] T. Delattre, C. Feuillet-Palma, L. G. Herrmann, P. Morfin, J.-M. Berroir, G. Fève, B. Plaçais, D. C. Glattli, M.-S. Choi, C. Mora, and T. Kontos, Nat. Phys. **5**, 208 (2009).
[33] J. Nygård, D. H. Cobden, and P. E. Lindelof, Nature (London) **408**, 342 (2000).
[34] M. Ferrier, T. Arakawa, T. Hata, R. Fujiwara, R. Delagrange, R. Weil, R. Deblock, R. Sakano, A. Oguri, and K. Kobayashi, Nat. Phys. **12**, 230 (2016).
[35] E. A. Laird, F. Kuemmeth, G. A. Steele, K. Grove-Rasmussen, J. Nygård, K. Flensberg, and L. P. Kouwenhoven, Rev. Mod. Phys. **87**, 703 (2015).
[36] T. Hata, R. Delagrange, T. Arakawa, S. Lee, R. Deblock, H. Bouchiat, K. Kobayashi, and M. Ferrier, Phys. Rev. Lett. **121**, 247703 (2018).
[37] J. C. E. Saldaña, R. Žitko, J. P. Cleuziou, E. J. H. Lee, V. Zannier, D. Ercolani, L. Sorba, R. Aguado, and S. D. Franceschi, Sci. Adv. **5**, eaav1235 (2019).
[38] V. Ambegaokar and A. Baratoff, Phys. Rev. Lett. **10**, 486 (1963).
[39] A. Levy Yeyati, A. Martín-Rodero, and E. Vecino, Phys. Rev. Lett. **91**, 266802 (2003).

[40] E. Vecino, M. R. Buitelaar, A. Martín-Rodero, C. Schönenberger, and A. Levy-Yeyati, Solid State Commun. **131**, 625 (2004).

[41] K. Mullen, Y. Gefen, and E. Ben-Jacob, Physica (Amsterdam) **152B**, 172 (1988).

[42] D. M. Badiane, L. I. Glazman, M. Houzet, and J. S. Meyer, C. R. Phys. **14**, 840 (2013).

[43] J. C. Cuevas, A. Martín-Rodero, and A. Levy Yeyati, Phys. Rev. B **54**, 7366 (1996).

[44] T. Novotný, A. Rossini, and K. Flensberg, Phys. Rev. B **72**, 224502 (2005).

[45] A. Eichler, R. Deblock, M. Weiss, C. Karrasch, V. Meden, C. Schönenberger, and H. Bouchiat, Phys. Rev. B **79**, 161407(R) (2009).

[46] A. Kadlecová, M. Žonda, and T. Novotný, Phys. Rev. B **95**, 195114 (2017).

[47] A. Kadlecová, M. Žonda, V. Pokorný, and T. Novotný, Phys. Rev. Applied **11**, 044094 (2019).

[48] R. Žitko, NRG LJUBLJANA—Open source numerical renormalization group code (2014), http://nrgljubljana.ijs.si.

[49] R. Žitko and T. Pruschke, Phys. Rev. B **79**, 085106 (2009).

[50] S. Y. Müller, M. Pletyukhov, D. Schuricht, and S. Andergassen, Phys. Rev. B **87**, 245115 (2013).

[51] J. Basset, A. Y. Kasumov, C. P. Moca, G. Zaränd, P. Simon, H. Bouchiat, and R. Deblock, Phys. Rev. Lett. **108**, 046802 (2012).

[52] A. Kaminski, Y. V. Nazarov, and L. I. Glazman, Phys. Rev. Lett. **83**, 384 (1999).

[53] A. Kaminski, Y. V. Nazarov, and L. I. Glazman, Phys. Rev. B **62**, 8154 (2000).

[54] J. Paaske, A. Rosch, J. Kroha, and P. Wölfle, Phys. Rev. B **70**, 155301 (2004).

[55] D. Averin and A. Bardas, Phys. Rev. Lett. **75**, 1831 (1995).

[56] C. W. J. Beenakker and H. van Houten, Phys. Rev. Lett. **66**, 3056 (1991).

[57] D. G. Olivares, A. L. Yeyati, L. Bretheau, C. O. Girit, H. Pothier, and C. Urbina, Phys. Rev. B **89**, 104504 (2014).

[58] B. Hiltscher, M. Governale, and J. König, Phys. Rev. B **86**, 235427 (2012).

[59] L. Dell'Anna, A. Zazunov, and R. Egger, Phys. Rev. B **77**, 104525 (2008).

[60] B. Lamic, J. S. Meyer, and M. Houzet, Phys. Rev. Research **2**, 033158 (2020).

[61] Y. N. Demkov and V. I. Osherov, Sov. Phys. JETP **26**, 916 (1968), http://jetp.ac.ru/cgi-bin/e/index/e/26/5/p916?a=list.

[62] M. Houzet, J. S. Meyer, D. M. Badiane, and L. I. Glazman, Phys. Rev. Lett. **111**, 046401 (2013).